Vacuum 123 (2016) 103–110

Contents lists available at ScienceDirect

Vacuum

journal homepage: www.elsevier.com/locate/vacuum

Atomic layer deposition process optimization by computational fluid dynamics

Zhang Deng [a], Wenjie He [a], Chenlong Duan [a], Bin Shan [b], Rong Chen [c, *]

[a] State Key Laboratory of Digital Manufacturing Equipment and Technology, School of Mechanical Science and Engineering, Huazhong University of Science and Technology, Wuhan, Hubei, PR China
[b] State Key Laboratory of Material Processing and Die & Mould Technology, School of Materials Science and Engineering, Huazhong University of Science and Technology, Wuhan, Hubei, PR China
[c] State Key Laboratory of Digital Manufacturing Equipment and Technology, School of Mechanical Science and Engineering, School of Optical and Electronic Information, Huazhong University of Science and Technology, Wuhan, Hubei, PR China

ARTICLE INFO

Article history:
Received 14 July 2015
Received in revised form
9 October 2015
Accepted 20 October 2015
Available online 23 October 2015

Keywords:
Atomic layer deposition
Dynamic flow
Quantitative
Gas velocity

ABSTRACT

This paper presents a computational fluid dynamics model to optimize atomic layer deposition (ALD) process, in which the temperature, precursor mass fraction, mass flow and pressure have been quantitatively analyzed by combining surface chemical reactions with species transport. Simulation results show that the higher temperature increases the growth rate and accelerates the surface deposition process, yet has little impact on precursor distribution in the entire chamber. Both computational and experimental results reveal that precursor concentration is the critical parameter which affects the cycle time and the precursor mass. The gas velocity, depended by the mass flow rate and chamber pressure, is the determinant factor for minimizing the cycle time. Moreover, quicker diffusion and homogeneous distribution resulted from low pressure and high mass flow rate facilitate the optimization of the ALD process. This quantitative model has been verified by experiments under different fluid conditions, which could provide instructive guidance to optimize deposition process in a large pressure range.

1. Introduction

Atomic Layer Deposition (ALD) is a powerful thin film deposition technique based on sequential self-terminating surface reactions [1–3]. The self-limiting nature of the precursor chemisorption in an ideal ALD process enables precise control of film thickness, as well as nice conformality and uniformity over large areas [4,5]. Recently, ALD has attracted much attention in the fields of microelectronics, optoelectronics, renewable energy, *etc.* [4,6,7]. One drawback of the ALD process, however, is the relatively low growth rate. To speed up the ALD process and lower the cost, it is necessary to reduce ALD cycle time and promote precursor usage by improving reactor structure and developing corresponding processes [8–10].

To date, conventional methods to optimize ALD processes are usually based on massive experiment runs [8,9,11–16]. Although some previous literature [11–13] have discussed the ALD growth among pressure, temperature and precursor materials respectively, the quantitative correlation study of process parameters is limited under particular reactor geometry. On the other hand, numerical modeling is an effective method to study the multiple operational parameters of ALD processes. There are three major types of quantitative simulations on ALD processes: microscopic simulation, theoretical derivation and equipment scale numerical simulation. Microscopic atomic scale simulations such as kinetic Monte Carlo methods have been utilized to calculate precursor transport and surface deposition on high aspect ratio substrates [17]. These microscopic methods, nevertheless, are restricted to small scales of space and time (usually within several micrometers/microseconds), and need a rather long time to complete calculations. Mathematical methods from theoretical derivations primarily focus on the calculation of the thermodynamic equilibrium states [18,19]. The computational fluid dynamic (CFD) simulations have been explored in equipment scale to analyze steady flow information of temperature distribution, pressure gradient, precursor concentration, *etc.* [20–25]. The quantitative optimizations of these process parameters require a comprehensive dynamic model that combines microscopic surface reactions in the reactor scale. Yuan's group has developed a quantitative numerical model with detailed

* Corresponding author.
E-mail address: rongchen@mail.hust.edu.cn (R. Chen).

http://dx.doi.org/10.1016/j.vacuum.2015.10.023
0042-207X/

surface reaction mechanisms to study the influences of temperature and precursor distributions on deposition rate at low pressure (0.1 Torr) [26,27]. The wide range of chamber pressures from vacuum (0.1 Torr) to atmospheric (760 Torr) conditions is chosen, yet the analysis on quantitative relationships between process parameters and the deposition efficiency is rarely reported. Exploring process operated under ambient pressure conditions will further expand the cognition of ALD processes in engineering.

In the present work, the influences of the temperature, precursor mass fraction, mass flow rate and pressure on the dynamic process optimization have been explored with a quantitative numerical model. The connection of process parameters with the deposition efficiency has been quantitatively discussed. The precursor concentration and gas velocity are the determinant factors for process optimizations. Experiments with different fluid conditions (precursor mass fraction, mass flow rate and pressure) have been conducted to support the model simulation results. This quantitative model combining surface chemistry and fluid dynamics would be instructive for both process optimization and reactor designs.

2. Methods

2.1. System description

Simulations on the study of operational parameters are verified by experiments on a bottom conductive heating reactor (inner diameter: 80 mm, height: 10 mm) as shown in Fig. 1a. The bottom heating reactors of this type are widely used in research laboratories due to their compact size and effective gas delivery. The entire system consists of five parts: precursor dosing hold-cells, the gas manifold, the closed chamber, integrated quadrupole mass spectrometer and pumping system (Fig. 1b). Though the pressure of gas mixture which contains precursor and carrier gas is monitored by a vacuum gauge (Edwards APGX-H-NW25), the precise amount of precursor could not be calculated from this total gauge pressure [8,9]. In order to solve this problem, hold-cells are designed to provide quantitative precursor dose which is very important to perform experimental verification in our equipment. The hold-cells measure the partial pressures of all species with *in-situ* quadrupole mass spectrometer of AMETEK Dycor (LC-D200). The partial pressure difference before and after precursor dosing represents the amount of precursor molecules pulsed into the chamber. The precursor molecules are injected into the reactor by switching off valves in the precursor dosing hold-cells. After the hold cell is pumped down to 1 Torr pressure, the thread valve is opened and other valves are closed, and then precursor molecules diffuse from precursor bottle to the hold cell. Precursor is taken out from the hold cell by a small amount of nitrogen gas (20 sccm), then is diluted with 500 sccm nitrogen again, finally fills into the manifold of the reactor. The amount of precursor molecules could be precisely controlled into the reactor regardless of the chamber pressure. In the experiment, the lowest dose amount is represented by the minimal dose time for the saturated ALD chemical adsorption. The minimal purge time is defined as the shortest time to completely remove the reactant and by product molecules from the reactor without overlap of the other precursor.

2.2. CFD model description

The CFD model is chosen to analyze these quantitative indicators by solving the conservation equations for mass, momentum, and energy [20–22]. The surface reaction is incorporated with the conventional dynamic flow for analyzing the velocity distribution and precursor concentration. The surface coverage represents the percentage of replaced species on the surface. Once the surface coverage reaches 100%, the value of consumed precursor gets the minimum for a completed ALD half reaction. In our study, the minimal dose time is represented by the shortest pulse time during which precursor molecules diffuse from the inlet to the boundary layer and adsorb on the substrate surface. The minimal purge time is defined as time interval in purging stage that the residual precursor mass fraction or molar fraction of gas mixture decrease to lower than 1.0×10^{-6} on the entire reactor. The optimizations of the cycle time are critical to improve the throughput and reduce precursor waste. Static chemical kinetics in surface exchange process is described by the Arrhenius expression. The physical parameters of all the associated chemical species and gas mixtures are listed in Table 1 (in Appendix).

In fluid dynamics theory, species distribution is comprised of the boundary layer and volume distributions [12]. In the boundary layer, the flow stream begins to stagnate and precursors contribute to the surface reaction. Once the gas molecules get into the boundary layer, the velocities decrease sharply and reach zero at the substrate surface. The boundary layer is an important media that links the macroscopic process parameters and the microscopic

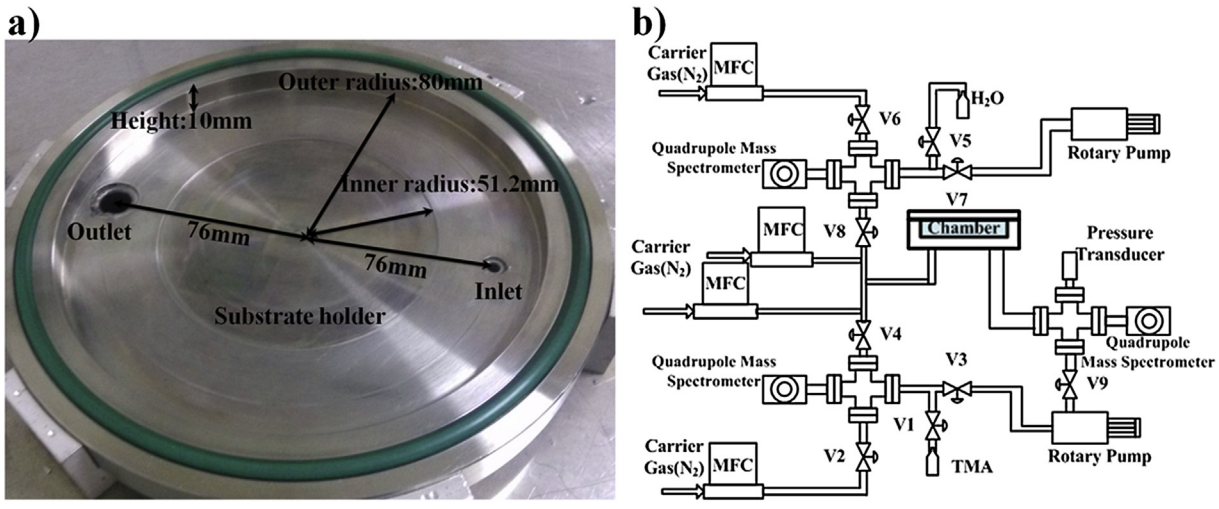

Fig. 1. a) The picture of reaction chamber with actual dimension; b) the schematic of hold-cells integrated ALD system.

Table 1
Physical parameters of chemical species by the quantitative calculations.

	Species	Standard state enthalpy [J/kmol]	Standard state entropy [J/kmol-k]	Molecular weight [kg/kmol]
1	Al−OH*	3.89E+07	183587.5	44.01
2	$Al(CH_3)_3$	−8.49E+07	350149.3	72.09
3	$AlOAl(CH_3)_2$*	5.34E+07	323887.9	100.05
4	CH_4	−7.49E+07	186040.1	16.04
5	Al−CH_3*	8.263E+07	253895.8	42.02
6	H_2O(vapor)	−2.42E+08	188696.4	18.02
7	N_2	0	191494.8	28.01

The asterisk indicates the avtive species of the surface.

surface chemical reactions. The thickness of the boundary layer is within a few millimeters regardless of mass flow rates. According to the transport theory, mass flux of precursor dose includes chamber volume flux, unreactive wall surface flux, and reactive surface flux. The calculation of total precursor mass pulsed into the reactor can be described as

$$\begin{aligned} m_{precursor} &= \left(\iint N_{precursor}dS + \iiint \rho_{precursor}dV\right)dt \\ &= \int_0^{t_{pulse}} \left(\int \left(\int D_{co}H_{BL}dc_{precursor} \right) dS \right. \\ &\quad \left. + \int C_{bulk}dV \right) dt \propto \boldsymbol{F}(\boldsymbol{p},\boldsymbol{f},\boldsymbol{c}), \end{aligned} \tag{1}$$

here $N_{precursor}$ is the flux of precursor in unit surface area, $\rho_{precursor}$ is the gas density of precursor, D_{co} is the diffusion coefficient, H_{BL} is the boundary layer thickness, $c_{precursor}$ is the concentration in the boundary layer, C_{bulk} is the concentration in the volume, p is the chamber pressure, f is the mass flow rate, c is the precursor mass fraction at the inlet. The surplus precursor molecules of volume flux and unreactive wall surface flux in the chamber will be purged away, while the molecules in the boundary layer contribute to the film growth. The simulations focus on fluid processes' key factors which determine the fluid status in the boundary layer.

3. Results and discussion

3.1. Influence of temperature distribution

The increase of the temperature accelerates the surface deposition in ALD process. At higher temperature, the decreased the growth rate is attributed to the enhanced desorption of the surface species [11,12,27]. Moreover, temperature distribution between the walls improves gas molecules movement by the thermophoretic force which generates longitudinal motion of gas molecules in the dynamic process.

The simulation results in Fig. 2 show the correlations of surface deposition rates and TMA mass fraction for pulsing process at 100 °C, 170 °C, and 250 °C, respectively. The mass changing of solid species O<s> deposited in TMA half reaction presents the instant deposition rate on the substrate. The black dotted lines in Fig. 2 show temperature effect on surface reactions and precursor distribution in dynamic flow. The growth rate (nm/cycle) is sensitive to the substrate temperature, and reduces at high temperature due to precursor desorption. The deposition rate of O<s> ($kg/m^2 \cdot s$) has little difference with temperature from 100 °C to 250 °C, however the residual time for surface coverage decreases from 90 ms to 50 ms. The deposition rate of O<s> is an order of magnitude smaller than that in the report [27] because of lower precursor concentration in our simulations. Thereafter, despite the increase of TMA mass fraction, the deposition rate turns to zero and the surface growth process finishes. Although surface deposition is dependent on temperature, TMA concentrations at substrate and middle volume are the same with temperature from 100 °C to 250 °C. Before the surface getting saturated, the deposition rate rises with the increase of precursor concentration. Then the growth rate will be largely restrained, once the surface sites are fully taken by nonreactive surface species. After the reactive surface species are totally substituted, the deposition rate turns to zero. The precursor concentration in the boundary layer is relatively smaller than that in the chamber volume. Higher temperature enhances the growth rate and accelerates surface deposition processes. Nevertheless, precursor distribution near the substrate and in the chamber volume remains the same value under different temperatures. With different substrate temperatures at the same fluid conditions, precursor gradient in space could be ignored.

3.2. Influence of precursor mass fraction

As mentioned above, the precursor concentration in the boundary layer is a part of the precursor mass influx into the chamber. Higher concentration in the boundary layer gets faster diffusion and adsorption in the surface reaction, yet leads to more unreacted precursors. Based on the self-limiting nature of the ALD, precursor molecules forms a monolayer on the substrate, and excess ones will be taken away by the purge gas. As shown in Fig. 3, under the same pressure and constant mass flow rate, lower precursor mass fraction requires longer dose time, especially at the precursor mass fraction below 1.0%. In this region, the consumed precursor mass determined by both precursor concentration and dose time will increase obviously. When the precursor mass fraction between 1.0% and 2.0%, the dose time decreases as precursor concentration increases. When the precursor mass fraction is higher than 2.0%, increasing concentration has hardly any contribution to species diffusion, thus the dose time is nearly a constant. In such a situation, however, larger concentration causes more precursor wastes. Consequently, the optimum precursor mass fraction ranges from 1.0% to 2.0% considering both minimization of dose time and precursor mass. Similar trends of the minimal dose time are observed under different pressures. A set of doable experiments on the relationship of the minimal dose time and the precursor mass fraction has been performed at 500 sccm mass flow and 600 Torr. The trends of such experiments are consistent with the simulation results as shown in Fig. 3. Furthermore, the relationship between the pressure and the minimal dose time needs to be analyzed jointly with the mass flow rate. Quantitative experiments on validation of pressures at constant precursor mass fraction will be discussed in the next section.

The minimal dose time is obtained at 3 Torr and 10 Torr in Fig. 3. At less than 10 Torr pressure, the states of dynamic precursor distribution are the same ones. The minimal dose time increases correspondingly as the pressure increases. Higher precursor mass fraction leads to more effective diffusion and shorter pulse time than those of low precursor mass fraction. Though higher precursor usage is obtained, long dose time is required with precursor

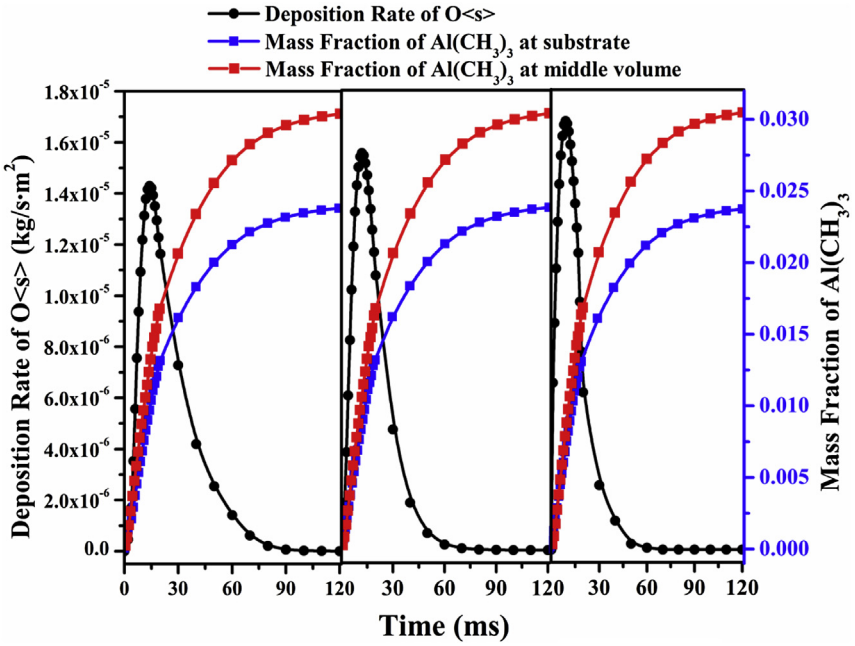

Fig. 2. Surface deposition rate of O<s> and TMA mass fraction distributions in pulse process with 10 Torr, 500 sccm at 100 °C, 170 °C and 250 °C.

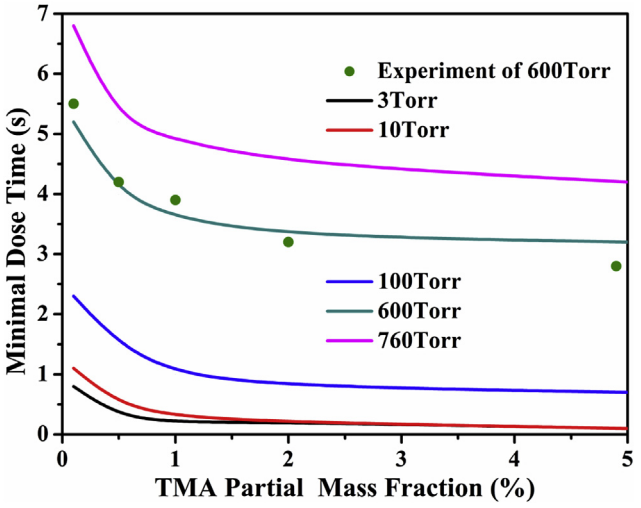

Fig. 3. Precursor dose time with different precursor mass fractions at several pressures and its experimental verification at 500 sccm and 600 Torr.

concentration lower than 1%, which is undesired for cycle time optimization. From high precursor usage perspective, the pressures below 10 Torr are better. The maximum TMA usage at vacuum in the given chamber is nearly 10%, which is relatively high compared to some other vacuum processes with either flow tube chamber [12] or bottom heating reactor [27]. Although using a particular source of TMA in this study, the precursor usage of other materials could be calculated with the corresponding physical and chemical parameters.

3.3. Influences of mass flow and pressure

Precursor distributions in the volume and the boundary layer are largely depended on the geometry and process conditions. The changes of each fluid parameter will result in different precursor distributions. To optimize the process and precursor usage, wide ranges of ALD fluid conditions (mass flow rate, pressure, precursor mass fraction) have been chosen. Specifically, the mass flow rate is between 500 and 5000 sccm, the pressure is between 10 Torr and 760 Torr, and the precursor mass fraction is between 0.1% and 5.0%.

The simulation results in Fig. 4 indicate that gas velocity, determined by mass flow rate and pressure, plays a major role on precursor distribution in the entire chamber. To explore the trend of cycle time by different gas velocities, a series of simulations are summarized with different mass flow rates and pressures under a constant precursor concentration. As shown in Fig. 4a, in terms of overall trend, the minimal dose time decreases with the mass flow rate increasing. With the reduction of pressure, the minimal dose time decreases gradually to a constant value eventually. The minimal dose time is jointly determined by the mass flow rate and the pressure. Under these vacuum conditions, the minimal dose time turns to a small value and changes slightly under different mass flow rates. Within the entire pressure range studied here, the minimal precursor consumption is lowest and constant below 10 Torr. The lower vacuum pressure leads to higher gas velocity and quicker diffusion, which results in effective optimization of ALD cycle time. This explains why a large number of ALD experiments are performed at the pressure below 10 Torr (lower to 0.1 Torr). While at high pressure near atmospheric conditions, both the gas velocity and the mean free path of molecules decrease, and then the mass flow rate tends to be more significant role in the decreasing of the cycle time. When the mass flow rate is lower than 5000 sccm, the minimal dose time is slightly affected with the increasing of gas velocity. In such a situation, laminar flow presents the irregularity. When the mass flow rate is higher than 5000 sccm, the minimal dose time tends to be a constant, and the system status turns to more complicated. In this region, higher mass flow rate has little contribution to improve precursor diffusion. Since the pulse and purge processes have the similar characteristic in the boundary layer, the adsorption in the pulse process and desorption in the purge process (Fig. 4b) follow the same trends as shown in Fig. 4a.

To validate the influence of mass flow rate on the ALD process, experiments are conducted with the mass flow rate varying from 500 sccm to 5000 sccm with 760 Torr pressure. As shown in Fig. 4c,

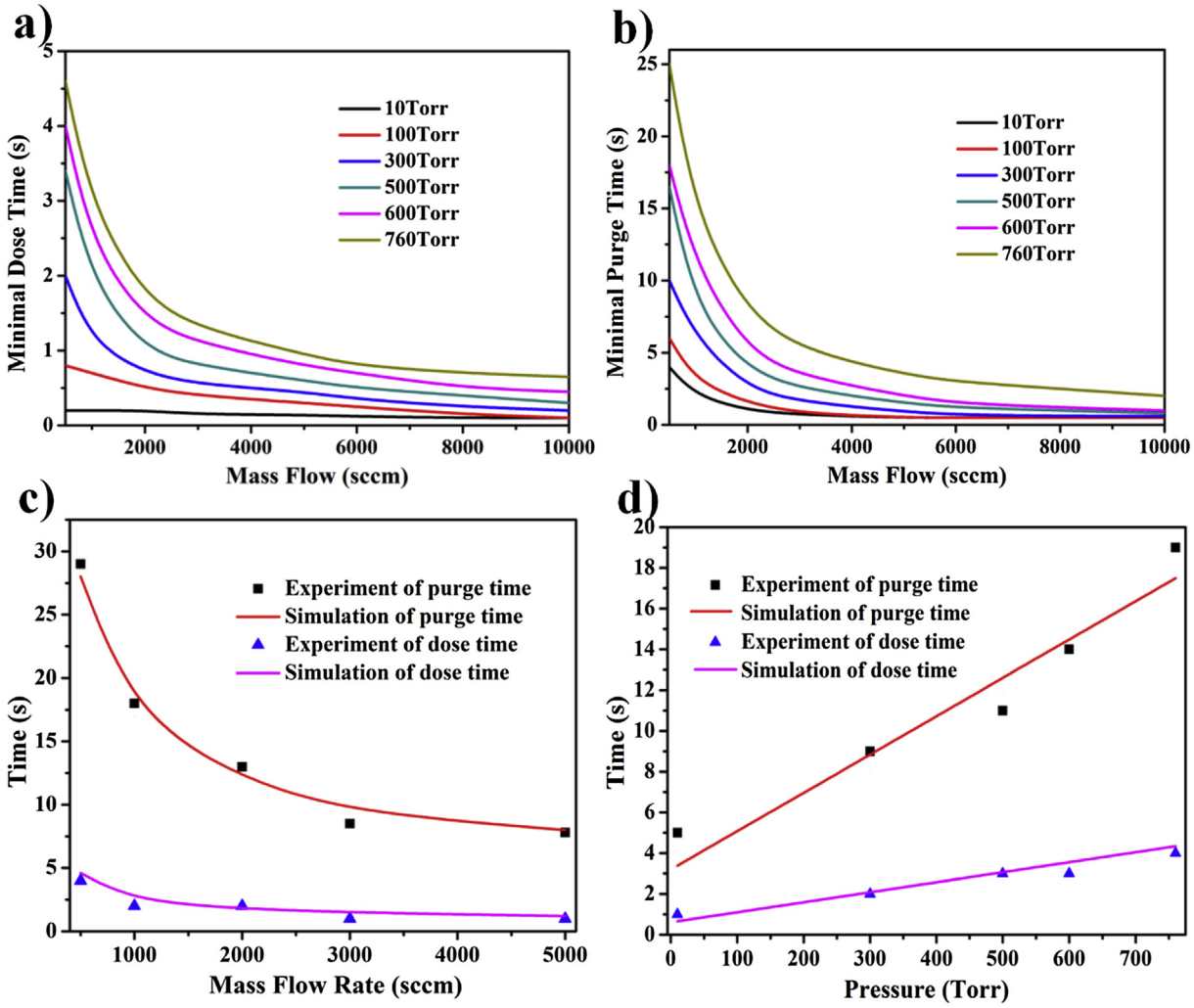

Fig. 4. a) The minimal precursor dose time simulation results; b) the minimal purge time simulation results; c) simulations and experiments comparison of the minimal dose and purge times at 760 Torr; d) simulations and experiments comparison of the minimal dose and purge times at 1000 sccm.

the experimental values are in a good agreement with the simulation predictions. Similarly, other experiments are carried out at the pressure range from 10 Torr to 760 Torr under constant 1000 sccm mass flow rate, to indicate that the minimal dose time is linear with the pressure. While the diffusion enhances greatly at low pressure, the dose time reaching 100% coverage decreases to 0.1 s at pressure lower than 10 Torr. Relatively better minimizations of dose and purge times are obtained at this pressure range. Although high gas velocity flow could be obtained at low pressure and high mass flow rate respectively, the status of fluid flow is different.

From the calculation of Reynolds number, fluid flow stays in laminar at different pressures. Although the cycle time changes linearly, the transient fluid status as pressure increasing from vacuum to atmospheric pressure changes irregularly. Similar to the influence of precursor concentration, the minimal value of cycle time is available at 10 Torr, and keeps the same at low vacuum pressure (0.1 Torr−10 Torr). In this situation, the regular laminar flow enables species rapid and uniform distribution. While at sub-atmospheric (500 Torr−760 Torr), the convection becomes the leading factor for irregular flow. To compare these fluid statuses, the velocity vectors at vacuum and high pressure conditions are shown in Fig. 5 respectively. As Fig. 5a shows, the irregular flow appears in the entire chamber at high pressure. Under the vacuum condition, the velocity vectors are uniformly distributed in the chamber as a laminar flow shown in Fig. 5b. With larger gas density and shorter molecular mean free path under higher pressure, the convection plays a greater impact on precursors' distribution near the substrate. While increasing the mass flow rate at sub-atmospheric pressure, the system tends to be irregular status which affects greatly on precursor distribution in the boundary layer. In short, high velocity at low pressure and high mass flow rate facilitate ALD reactions because of the faster diffusion and homogeneous distribution near the substrate surface.

In fluid theory, the average velocity is parallel to the substrate, which is the bulk velocity of stream v, and it can be derived from the formula of flow conductivity and presented with the mass flow rate and pressure. According to the summary of dose and purge time results in Fig. 4, the cycle time could be determined by both pressure and mass flow rate as equation (2)

$$T_{cycle} = t_{pulse} + t_{purge} = \frac{C}{v+E} + D = \frac{AP}{K(\varphi + B)} + D, \quad (2)$$

here T_{cycle}, t_{pulse}, t_{purge} are the cycle time, dose time and purge time of the ALD process respectively, A, B, C, D, E and K are constants

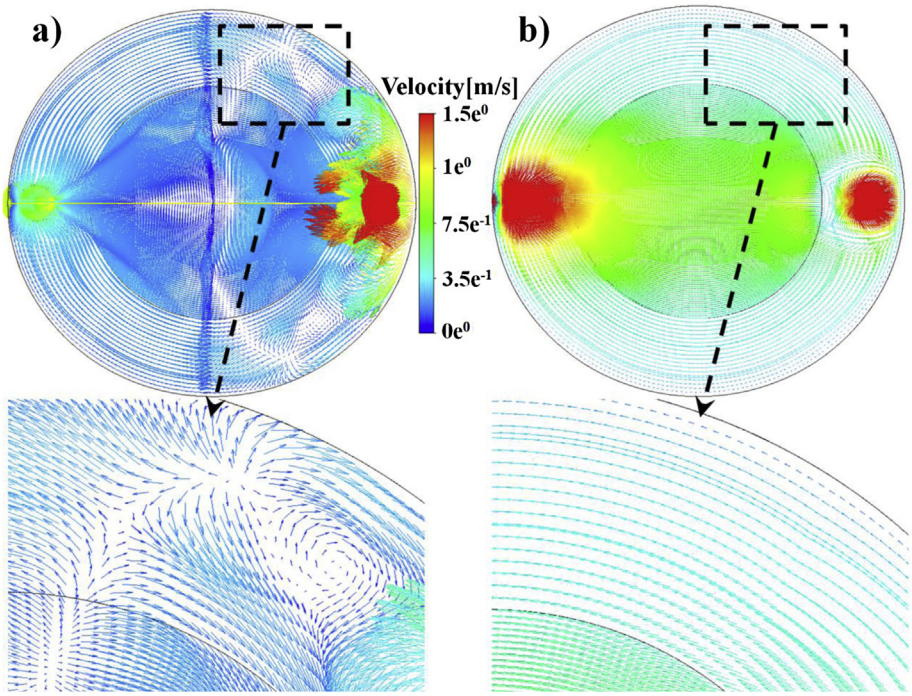

Fig. 5. Fluid distribution a) irregular flow at atmospheric pressure with 760 Torr and 500 sccm; b) regular laminar flow at vacuum pressure with 10 Torr and 500 sccm.

concluded from simulation results in Fig. 4. The cycle time is associated with the average gas velocity, which is proportional to mass flow rate, and inversely proportional to pressure. Concluded from equation (2), there is a strong correlation between the cycle time and gas velocity with the media of mass flow rate and pressure. Therefore, under the given temperature, low pressure P and high mass flow rate φ result in large velocity which shortens the cycle time for each monolayer formation. The system stays at the transition states of irregular laminar flow. These fluid flow conditions are better choices for production application in an open environment. Under vacuum conditions (<500 Torr), species diffusion is strengthened and laminar flow becomes steady. Thus, faster diffusion and better species transport make these conditions suitable for large number of ALD processes.

Process efficiency and precursor utilization are improved with smaller reactor volume. However, the smaller geometry may end up with non-uniform precursor distribution. For high throughput required applications like solar cells, small chamber and quick process need to be placed at atmospheric environment. For high quality thin film requirement, the vacuum condition needs to be chosen in a closed chamber. The quantitative relationship between chamber structure and process could provide instructive information for reactor and process designs. Some structural designs like shower head in the gas inlet are also estimable for efficiency improvement. Meanwhile, chemistry kinetics with the planar substrate in this quantitative model could be easily expanded to the large area deposition, even with flexible or rolled ways in mass production.

4. Conclusions

With the quantitative numerical model, the temperature, precursor mass fraction, mass flow rate and pressure are analyzed for ALD process efficiency. Although higher temperature increases the growth rate and accelerates the surface deposition processes, it has little impact on precursor distribution in the entire chamber. Precursor gradient resulted from the temperature difference could be neglected. Quicker diffusion and shorter pulse time could be available at higher precursor mass fraction. At low pressure (0.1 Torr–10 Torr), species distribution turns to be the same and effective state. By summarizing the results from simulations and experiments, a balance between shorter dose time and better precursor usage is necessary based on an optimum range of precursor mass fraction. Simulations and experimental results reveal that gas velocity decided by the mass flow rate and chamber pressure is the determinant factor for minimization of the cycle time. While increasing the mass flow rate at sub-atmospheric pressure, the system tends to be irregular status which affects greatly on precursor distribution near the substrate. Thus, quicker diffusion and homogeneous distribution resulted from low pressure and high mass flow rate facilitate the optimization of the ALD process. This quantitative model combining surface chemistry and fluid dynamics is informative to improve the process at large scale of pressure, and effective to replace massive experiment runs in production applications.

Acknowledgments

The authors would like to acknowledge Aoming Li from AMETEK lab for mass spectrum detection, as well as technology support by the Analytic Testing Center of HUST. This work is supported by the National Basic Research Program of China (2013CB934800), the National Natural Science Foundation of China (51575217 and 51572097), the Hubei Province Funds for Distinguished Young Scientists (2015CFA034 and 2014CFA018) and the State Key Laboratory of Digital Manufacturing Equipment and Technology Funding (DMET2015A01). Rong Chen acknowledges the Thousand Young Talents Plan, the Recruitment Program of Global Experts, and the Program for Changjiang Scholars and Innovative Research Team in University (IRT13017).

Appendix A. Supplementary material

Supplementary material related to this article can be found at http://dx.doi.org/10.1016/j.vacuum.2015.10.023.

Appendix

In this study, the activation energy and pre-exponential factor of chemical reactions are taken from Arrhenius expression for Al_2O_3 thin films with trimethylaluminum (TMA) and water as precursors. Other precursors and thin film materials with specific parameters of chemistry kinetics could also be analyzed by fluid kinetics from the numerical model. With fundamental surface theory, Si–O bond length of 1.6 Å is selected, and a value of site density is derived as $D = 5 \times 10^{14}$ molecules/cm^2, and the precursor mass for saturated monolayer growth is

$$m_A = \frac{D\pi r^2 M}{N_A}, \quad (3)$$

here r is the radius of the silicon wafer, M is the molar weight and N_A is Avogadro's constant. From equation (3), the minimal precursor mass of 4.699 μg is available to replace the surface sites completely.

Table 1 provides the values for the molecular weight (M), the standard state enthalpy, and the standard state entropy for each species considered in the model. The specific heat capacities at constant pressure (C_p) are calculated from kinetics theory.

The model is initialized with the mixture of N_2 carrier gas and precursors, and the temperature of gas mixture (Nitrogen + TMA) from the inlet is set to 298 K. The mass fraction of TMA in the mixture varies from 1×10^{-3} to 5×10^{-2}. The wall temperature distribution of the reactor model fits to the results of experimental measurement, and the reactive substrate surface is set to 443 K which is in the temperature window of Al_2O_3 ALD. As the continuous fluid flow in the ALD process is decided by the Knudsen number, the CFD calculation is fitted to this complicated situation. According to the Reynolds equation, there is laminar flow in vacuum condition and tends to be irregular when pressure increased.

As mentioned above, the minimal dose time is defined as the shortest pulse time of fully surface coverage by reactive species, which means the minimum consumption of precursor mass for a surface reaction. As illustrated in Fig. 6 (see Supplementary material), the surface coverage reaches near 80% at the transient of 0.5 s. At this moment, the percentage of exchanged species on substrate is presented in Fig. 6b. By contrast with Fig. 6a, the precursor distributions in the volume could not reflect the progress of surface reaction directly. The minimal dose time is measured by the combination of *in-situ* quadrupole mass spectrometer (QMS) and ellipsometer. QMS is integrated for species tracking at upstream and downstream of the reactor, while the ellipsometry is installed hanging above the top cover of the chamber for the real time thickness measurement at dose process. From the transparent windows on the top cover, the polarized light incident into substrate and reflect out to the chamber. The minimal dose time is represented by the shortest pulse time during which precursor molecules diffuse into the chamber and the saturated growth on the surface is finished. QMS could monitor the precursor dose mass and the reaction time from concentration tracking of precursors and by products species, while the growth thickness from the *in-situ* ellipsometry could represent the saturation of the film growth.

The minimal purge time means that the species concentrations of reactants and by products are lower than 1 ppm on the entire reactor wall. The purge time in simulation is selected as the mean value of minimum and maximum residual time of precursor species in the chamber. The minimal residual time selects the points on the outlet or the substrate as the amount tracking of residual molecules; while the maximal residual time selects the point at dead angle (Fig. 7a in Supplementary material). In the constant concentration pulse, the MFC's response time is 2.0 s. The delay of MFC is about 1.0 s in every switch (Fig. 7b in Supplementary material). These offsets have been amended in the reported experimental results. The reactant tracking from downstream QMS could be directly used to measure the purge time. When the QMS signal of 57 (TMA) sharply decrease to the baseline during a purge process, it represents this purge process completes with all the surplus precursor molecules be effectively wiped out. The time length in such progress is defined as the minimal purge time.

References

[1] R.L. Puurunen, Surface chemistry of atomic layer deposition: a case study for the trimethylaluminum/water process, J. Appl. Phys. 97 (2005) 121301–121352.
[2] R.L. Puurunen, W. Vandervorst, Island growth as a growth mode in atomic layer deposition: a phenomenological model, J. Appl. Phys. 96 (2004) 7686–7695.
[3] P. Poodt, D.C. Cameron, E. Dickey, S.M. George, V. Kuznetsov, G.N. Parsons, , et al.A. Vermeer, Spatial atomic layer deposition: a route towards further industrialization of atomic layer deposition, J. Vac. Sci. Technol. A 30 (2012) 010802.
[4] S.M. George, Atomic layer deposition: an overview, Chem. Rev. 110 (2010) 111–131.
[5] R.L. Puurunen, Growth per cycle in atomic layer deposition: a theoretical model, Chem. Vap. Depos. 10 (2004) 249–257.
[6] Y. Zhang, H.L. Lu, Y. Geng, Q.Q. Sun, S.J. Ding, D.W. Zhang, Impact of rapid thermal annealing on structural and electrical properties of ZnO thin films grown atomic layer deposition on GaAs substrates, Vacuum 103 (2014) 1–4.
[7] W.M.M. Kessels, M. Putkonen, Advanced process technologies: plasma, direct-write, atmospheric pressure, and roll-to-roll ALD, MRS Bull. 36 (2011) 907–913.
[8] R. Matero, A. Rahtu, M. Ritala, M. Leskela, T. Sajavaara, Effect of water dose on the atomic layer deposition rate of oxide thin films, Thin Solid Films 368 (2000) 1–7.
[9] T.J. Larrabee, T.E. Mallouk, D.L. Allara, An atomic layer deposition reactor with dose quantification for precursor adsorption and reactivity studies, Rev. Sci. Instrum. 84 (2013) 014102.
[10] E. Granneman, P. Fischer, D. Pierreux, H. Terhorst, P. Zagwijn, Batch ALD: characteristics, comparison with single wafer ALD, and examples, Surf. Coat. Technol. 201 (2007) 8899–8907.
[11] M.B.M. Mousa, C.J. Oldham, J.S. Jur, G.N. Parsons, Effect of temperature and gas velocity on growth per cycle during Al_2O_3 and ZnO atomic layer deposition at atmospheric pressure, J. Vac. Sci. Technol. A 30 (2012) 01A155.
[12] J.S. Jur, G.N. Parsons, Atomic layer deposition of Al_2O_3 and ZnO at atmospheric pressure in a flow tube reactor, ACS Appl. Mater. Interfaces 3 (2011) 299–308.
[13] M.B.M. Mousa, C.J. Oldham, G.N. Parsons, Atmospheric pressure atomic layer deposition of Al_2O_3 using trimethylaluminum and ozone, Langmuir 30 (2014) 3714–3718.
[14] J.W. Elam, M.D. Groner, S.M. George, Viscous flow reactor with quartz crystal microbalance for thin film growth by atomic layer deposition, Rev. Sci. Instrum. 73 (2002) 2981–2987.
[15] P. Vermont, V. Kuznetsov, E.H.A. Granneman, High-throughput solar cell passivation on in-line Levitrack ALD Al_2O_3 system-demonstration of process performance, in: Proceedings of the 26th European Photovoltaic Solar Energy Conference, Hamburg, Germany, 2011, pp. 1644–1647.
[16] E.H.A. Granneman, P. Vermont, V. Kuznetsov, M. Coolen, K. Vanormelingen, High-throughput, in-line ALD Al_2O_3 system, in: 25th European Photovoltaic Solar Energy Conference and Exhibition, Valencia, 2010.
[17] A. Venkattraman, A.A. Alexeenko, Direct simulation Monte Carlo modeling of metal vapor flows in application to thin film deposition, Vacuum 86 (2012) 1748–1758.
[18] R.A. Adomaitis, U.O. Maryland, Development of a multiscale model for an atomic layer deposition process, J. Cryst. Growth 312 (2010) 1449–1452.
[19] A.M. Lankhorst, B.D. Paarhuis, H.J.C.M. Terhorst, P.J.P.M. Simons, Transient ALD simulations for a multi-wafer reactor with trenched wafers, Surf. Coat. Technol. 201 (2007) 8842–8848.
[20] Z. Karim, Y. Senzaki, S. Ramanathan, J. Lindner, H. Silva, M. Dauelsberg, Advances in ALD equipment for sub-40nm memory capacitor dielectrics : precursor delivery, materials and processes, Electrochem. Soc. Trans. 16 (2008) 125–134.
[21] J.C.S. Kools, High throughput atomic layer deposition for encapsulation of large area electronics, Electrochem. Soc. Trans. 41 (2011) 195–201.
[22] N. Baguer, E. Neyts, S. Van Gils, A. Bogaerts, Study of atmospheric MOCVD of TiO_2thin films by means of computational fluid dynamics simulations, Chem.

Vap. Depos. 14 (2008) 339–346.
[23] S.H. Othman, S.A. Rashid, T.I.M. Ghazi, N. Abdullah, 3D CFD simulations of MOCVD synthesis system of titanium dioxide nanoparticles, J. Nanomat. 2013 (2013). Article ID 123256, 11 pages, http://dx.doi.org/10.1155/2013/123256.
[24] Q. Xu, R. Zuo, H. Zhang, Analysis of reaction kinetics and numerical simulation of GaN growth by MOCVD, J. Chem. Ind. Eng. 60 (2009) 384–388.
[25] A. Holmqvist, T. Torndahl, S. Stenstrom, Scale-up analysis of continuous cross-flow atomic layer deposition reactor designs, Chem. Eng. Sci. 81 (2012) 260.
[26] M.R. Shaeri, T.C. Jen, C.Y. Yuan, Improving atomic layer deposition process through reactor scale simulation, Int. J. Heat Mass Transf. 78 (2014) 1243.
[27] D.Q. Pan, L.L. Ma, Y.Y. Xie, T.C. Jen, C. Yuan, On the physical and chemical details of alumina atomic layer deposition: a combined experimental and numerical approach, J. Vac. Sci. Technol. A 33 (2015) 021511.